Assessment of physical and mechanical properties of concrete with carbon nanotubes pre-dispersed in cement

Elvys Dias Reis, Heron Freitas Resende, André Luis Christoforo, Rodrigo M. Costa, Fabrice Gatuingt, Flávia Spitale Jacques Poggiali, Augusto Cesar da Silva Bezerra

Assessment of physical and mechanical properties of concrete with carbon nanotubes pre-dispersed in cement

E. D. Reis[a,d], H. F. Resende[a], A. L. Christoforo[b], R. M. Costa[c], F. Gatuingt[d], F. S. J. Poggiali[a], A. C. S. Bezerra[e]

[a] Federal Center for Technological Education of Minas Gerais, Dept. of Civil Engineering, Belo Horizonte, Brazil.
[b] Federal University of São Carlos, Dept. of Civil Engineering, São Carlos, Brazil.
[c] Pontifical Catholic University of Minas Gerais, Dept. of Civil Engineering, Belo Horizonte, Brazil.
[d] Université Paris-Saclay, CentraleSupélec, ENS Paris-Saclay, CNRS, LMPS – Laboratoire de Mécanique Paris-Saclay, Gif-sur-Yvette, France.
[e] Federal Center for Technological Education of Minas Gerais, Dept. of Transport Engineering, Belo Horizonte, Brazil.

Corresponding author: Elvys Dias Reis
elvysreis@yahoo.com.br

Abstract

This research evaluates the physical and mechanical properties of concrete with carbon nanotubes (CNT–concrete), including compressive strength (*CS*), tensile strength (*TS*), static (E_s) and dynamic modulus of elasticity (E_d), water absorption (*WA*), porosity (*P*), bulk density (ρ_{ap}), weight loss (*WL*), ultrasonic pulse velocity (*UPV*), and electrical resistivity (*ER*). Specifically, this paper investigates the correlations between these properties and proposes quadratic regression models based on CNT contents to estimate them. For this, an extensive experimental campaign was carried out. As a novelty, CNT were pre-dispersed in the cement particles in isopropanol to produce the concrete, a proven effective process but used only pastes and mortars so far. Concrete samples were produced with CNT contents of 0% (as a reference), 0.05%, and 0.10% by weight of cement, with 30 cylindrical specimens measuring 100×200 mm being molded for each composition. The results revealed that including 0.05% CNT led to statistically significant results, such as reductions of up to 12% in *P* and 14% in *WA* and increases of up to 16% in *CS*, 29% in *TS*, and 3% at *UPV*. At 0.10% CNT, E_d showed up to 10% improvements, while *WL* increased to 28%. It was also shown that pre-dispersing powdered CNT in cement particles using an isopropanol medium is effective for use in concrete, but dispersing CNT in water is simpler, safer, and potentially more efficient, especially for industrial production. Another important conclusion was the identification of significant correlations between some properties, which varied with the amount of CNT added, suggesting the existence of a CNT saturation point. Furthermore, the regression models identified ideal CNT contents for *P*, *WA*, *CS*, *TS*, and *UPV*, ranging between 0.045% and 0.123% CNT. This research also points to the need for additional studies to improve the regression models's quality and thoroughly assess the benefits of incorporating CNT into concrete.

Keywords: Carbon Nanotubes; Cementitious Materials; Durability; Regression models; Sustainability.

1. Introduction

Concrete is a widely used construction material due to its low cost, versatility, and abundant raw materials [1,2]. However, with increasing demands for higher engineering standards, concrete with improved mechanical properties, durability, and environmental performance has become essential [3]. Conventional concrete has limitations regarding tensile strain, fracture toughness, and brittleness, restricting its application in specific structures [4,5]. Researchers have explored using additives and nanomaterials to overcome these limitations to enhance its performance [6,7].

In this sense, carbon nanotubes (CNT), cylindrical carbon structures with dimensions on the nanometric scale, are promising nanomaterials to improve concrete's physical and mechanical properties [8,9]. CNT are elongated fullerenes with outstanding mechanical properties and thermal and electrical conductivity, the main types used in concrete reinforcement being single-walled carbon nanotubes (SWCNT) and multi-walled carbon nanotubes (MWCNT) [10]. Incorporating CNT into concrete can significantly improve its mechanical properties, acting as bridges reinforcing the cementitious matrix [11] and further catalyzing the nucleation of hydration products to enhance the concrete's properties [12,13]. However, it is worth mentioning that achieving a uniform and effective CNT dispersion in concrete is crucial, as CNT tend to agglomerate due to van der Waals forces and hydrophobicity [14,15].

Several approaches are used to disperse CNT in cement matrices, the most common being mechanical stirring, magnetic stirring, surfactant addition, and sonication. The effectiveness of each one depends on the characteristics of the CNT and the medium in which they are being dispersed. Often, these methods are combined to achieve optimal dispersion, such as adding surfactant followed by ultrasonication, which can simultaneously deagglomerate and stabilize the CNT. The choice and optimization of these techniques are fundamental to the successful integration of CNT into cementitious matrices.

Marcondes and Medeiros [16] used a hierarchical analysis to examine twelve different methods of dispersing MWCNT in aqueous media, including adding various chemicals, for use in Portland cement concrete. The CNT used were NC 7000 in powder form and AQ 0301 in water-dispersed form, supplied by Nanocyl SA, Belgium. In all the experiments, the proportion of 0.3% CNT about the total volume of water was maintained. The solutions were prepared in test tubes and mechanically stirred before being sonicated at 40 kHz. It was revealed that sonication for extended periods (40–60 minutes) minimizes sedimentation, and microscopic observation proved essential to discern dispersion nuances not visibly detectable. The authors used three criteria to assess the CNT dispersion: turbidity, the diameter of the agglomerates, and decantation. The results showed that the sample with AQ 0301 had the best dispersion, indicating that the industrial dispersion process is notably superior to the laboratory alternatives tested. Although the samples with powdered CNT showed signs of agglomeration, the study provided valuable insights for refining dispersion techniques.

Rocha and Ludvig [17], in turn, analyzed the mechanical performance of Portland cement pastes with 0%, 0.05%, and 0.10% non-functionalized MWCNT. The process involved mixing CNT with approximately 30 ml of isopropanol and then sonication at 42 Hz for 30 minutes. Afterward, 300 grams of cement and 200 ml of isopropanol were added. This mixture was shaken at 500 rpm and sonicated for another 2 hours. After a 24-hour drying period to evaporate the isopropanol, the dry cement-CNT mixture was used for cement paste preparation. Tests conducted after a 28-day curing period showed that

incorporating 0.05% CNT resulted in a 50% increase in compressive and splitting tensile strengths.

In this context, researchers have studied the influence of adding MWCNT to conventional concrete employing different dispersion techniques, such as Carriço et al. [18] (sonication for 30 min + by surfactant addition, for powdered CNT; sonication for 45 min in 3 cycles of 15 min, for CNT in aqueous form), Parvaneh and Khiabani [19] (sonication with surfactant for 120 min + mechanical stirring), Hawreen et al. [20] (magnetic stirring with 40% of the water, CNT and surfactant + addition of the remaining 60% of water + magnetic stirring for 240 min + sonication for 30 min, for powdered CNT); Magnetic stirring in water with surfactant + sonication for 30–45 min, for CNT in aqueous form), Mohsen et al. [21] (sonication for 30 min + mixing for 60 min), Hassan et al. [22] (dispersion in water), Mohammadyan-Yasouj and Ghaderi [23] (magnetic stirring in water for 30 min + sonication for 60 min), and Irshidat [24] (dispersion in water and manual agitation + sonication for 20 min). Notably, the state of CNT (in powdered or aqueous form) holds significance as it directly impacts dispersion methods. Thus, each study employs different combinations of the main techniques and concentrations (up to 2%), reflecting the diversity of approaches and the lack of a standard method in the area. This fact indicates a field of research still under development, where optimizing the dispersion of CNT in Portland cement-based materials, especially concrete, remains a topic open to innovation and improvements in existing methodologies.

Despite the extensive research conducted on concrete with carbon nanotubes (CNT–concrete) worldwide, standardized characterization methods for evaluating CNT's influence on concrete's properties still need to mature, and the field remains in the exploratory stage [25]. Moreover, laboratory testing can be costly and time-consuming. In this context, the correlation between the concrete's physical, mechanical, and durability properties and statistical regression models is essential to face these challenges [26]. This correlation allows for a deeper understanding of the complex relationships between these properties, such as compressive strength, tensile strength, modulus of elasticity, and durability [27]. Through statistical regression models, it is possible to establish mathematical relationships that enable engineers to predict the buildings' structural behavior based on the concrete's properties, including load capacity, deformation, durability, and useful life [28]. Furthermore, regression models are applied to optimize concrete mixes, determining the ideal ingredients' combination, the aggregates' proportion, cement content, and additions to achieve desired properties such as strength, durability, and cost-effectiveness [29]. This correlation also plays a crucial role in developing standards in the construction industry based on empirical and scientific data related to the concrete's characteristics and contributing to defining limits, acceptance criteria, and guidelines for use [30].

With this perspective, this paper aims to assess the CNT–concrete's physical and mechanical properties, namely, compressive strength, tensile strength, static and dynamic modulus of elasticity, water absorption, porosity and bulk density, weight loss, ultrasonic pulse velocity, and electrical resistivity. Given the importance of finding methods of dispersing nanomaterials that can be applied on an industrial scale, this research brings as a novelty the application of CNT pre-dispersed in cement particles in the production of concrete, a proven effective process in previous research with pastes and mortars [13,17]. In other words, the CNT are not dispersed directly with the other constituents of the mixture when the concrete is made, as is commonly done by the scientific community. The effectiveness of this method is tested by comparing the variations in mechanical and physical properties obtained in this study with those in the literature. In addition, the correlation between the properties above is presented, and quadratic regression models

are proposed to estimate them based on CNT content. It is worth mentioning that this work is part of research on the bonding behavior between steel bars and CNT–concrete, providing partial results and perspectives that will be useful in continuing investigations.

2. Materials and methods

2.1. Materials

The materials used in the concrete production were:

(i) Brazilian Type CPV-ARI RS Portland cement [31]—cement with low additions content in its chemical composition and a high fineness degree—produced by Holcim, with physical and mechanical properties shown in Table 1. This cement is comparable to CEM I of the EN 197-1 standard [32].
(ii) natural sand (fine aggregate, FA) with a 2.75 fineness modulus and 2.4 mm maximum diameter, characterized according to ABNT NBR NM 248 [33], and 2.632 g/cm^3 specific gravity, characterized according to ABNT NBR 9776 [34];

Table 1. CPV-ARI Portland cement's physical and mechanical properties.

Test type		Characteristic		Reference	Limit
Specific area—Blaine (cm^2/g)		4620		NBR 16372 [35]	≥ 3000
Setting time	Start	135		NBR 16607 [36]	≥ 60
	End	205		NBR 16607 [36]	≤ 600
Compressive strength (MPa)		1 day	19.6	NBR 7215 [37]	≥ 14.0
		3 days	31.8	NBR 7215 [37]	≥ 24.0
		7 days	41.3	NBR 7215 [37]	≥ 34.0
		28 days	52.4	NBR 7215 [37]	-

(iii) gneiss gravel (coarse aggregate, CA) with a 4.92 fineness modulus and 9.5 mm maximum diameter [33], and 2.646 g/cm^3 specific gravity [34];
(iv) MWCNT (only for CNT–concrete samples) selected from CTNano, Brazil, synthesized by chemical vapor deposition (CVD), with estimated lengths between 5 and 30 μm, external diameter between 10 and 30 nm, and purity greater than 93%—complete specifications described in the nanomaterial datasheet [38]. The isopropanol used to disperse the CNT was the EMFAL's absolute grade—detailed specifications in the alcohol datasheet [39];
(v) superplasticizer (SP) and hydration stabilizer (HS) additives in water suspension, whose specifications are in Table 2. The choice of a polycarboxylate-type SP is worth mentioning because the cement and calcium ions' alkaline medium directly influences nanomaterials' agglomeration. For example, Chuah et al. [40] used a polycarboxylate-type SP to disperse graphene oxide and obtained promising results.

Table 2. Superplasticizer and hydration stabilizer additives' properties.

Property	Superplasticizer	Hydration stabilizer
Name	Sika® ViscoCrete®–5800 FTN	Matchen stabilizer
Aspect at 25 ºC	Brown liquid	Blue liquid
pH	4.5 ± 1.0	3.5–5.5
Density at 25 ºC (g/cm^3)	1.07 ± 0.02	1.035–1.095
Suggested content	0.2%–2.0%	–

2.2. CNT dispersion

CNT were pre-dispersed on cement particles in an isopropanol medium. Fig. 1 presents an overview of the process. The method essentially consisted of three steps: (i) CNT and approximately 200 ml of isopropanol were added to a glass container, which was shaken at 10.000 rpm and sonicated on ultrasonic apparatus with 42 kHz frequency for 30 minutes; (ii) ten percent of the cement mass and another 200 ml of isopropanol were incorporated into the mixture, which was transferred to a plastic container and mechanically stirred and sonicated for additional 90 minutes; (iii) in a glass container, drying in an oven at 100±5 ºC for 24 hours, leaving only a visually homogeneous dry power of cement particles coated with CNT. The resulting dry mixture was then mixed with the remaining cement to prepare the CNT–concrete samples before adding water.

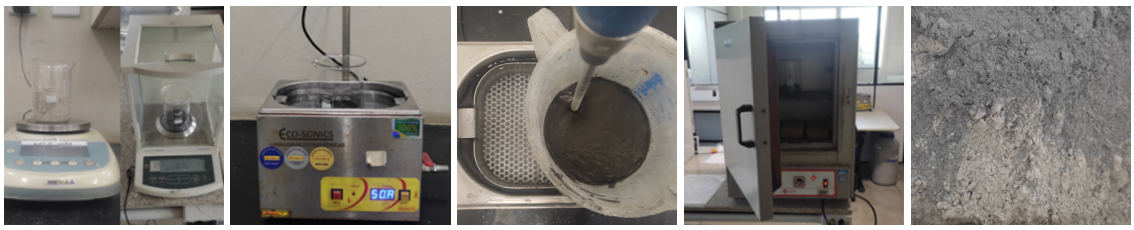

(a) (b) (c) (d) (e)

Fig. 1. CNT dispersion steps: (a) cement and CNT weighing; (b) CNT ultrasonication in isopropanol; (c) CNT and cement mechanical stirring in isopropanol; (d) oven drying of the mixture; (e) mixing of the dispersed CNT with the remaining cement.

The efficiency of this technique in concrete was compared with that of other methods presented in the literature, taking as a reference the variations in the mechanical and physical properties of CNT-concrete at 28 days, namely compressive strength, tensile strength, porosity, and ultrasonic pulse velocity.

2.3. Mixture compositions and specimen production

The concrete mixes in Table 3 were produced with a 0.53 water-to-cement (w/c) ratio, aiming for a S160 slump class and Group I compressive strength (30 MPa), following ABNT NBR 8953 [41]. The SP additive content of the sample with 0.10% CNT was adjusted to guarantee the concrete workability. The decision to opt for a more fluid concrete mix was driven by achieving better consolidation in areas with higher reinforcement concentrations, such as beam-column connections, where bond strength has critical importance. For the CNT–concrete samples, the CNT contents were limited to 0.05% ($CNT_{0.05}$) and 0.10% ($CNT_{0.10}$) by weight of cement (wc)—or 0.192 kg/m^3 and 0.384 kg/m^3, respectively—to prevent agglomeration issues [22]. Concrete samples without CNT ($CNT_{0.00}$) were also produced as a reference for comparative analysis.

Table 3. Concrete's mix proportions.

Mix	Cement (kg/m^3)	Aggregates (kg/m^3)		Water (kg/m^3)	Additives (kg/m^3)		CNT (%wc)
		FA	CA		SP	HS	
$CNT_{0.00}$	384	960	838	204	0.80	0.26	0.00
$CNT_{0.05}$	384	960	838	204	0.80	0.26	0.05
$CNT_{0.10}$	384	960	838	204	0.96	0.26	0.10

Fig. 2 provides an overview of concrete specimen production. The mixture was produced using a 120 L concrete mixer in three steps: (i) a small amount of water was added to moisten the mixer's inside surface; (ii) the aggregates were mixed with 60% of the total mixing water for three minutes; (iii) the cement (with or without CNT), SP and HS additives, and the remaining 40% of mixing water were added and mixed for additional five minutes. For each composition, 30 cylindrical specimens measuring 100×200 mm were molded in two steps and compacted manually. After 24 h, all the samples were de-molded and cured in saturated calcium hydroxide solution at 23±2 °C for 28 days, as recommended by ABNT NBR 5738 [42]. Five specimens were used to study the following properties: compressive strength, tensile strength, static and dynamic modulus of elasticity, water absorption, porosity and bulk density, weight loss, ultrasonic pulse velocity, and electrical resistivity.

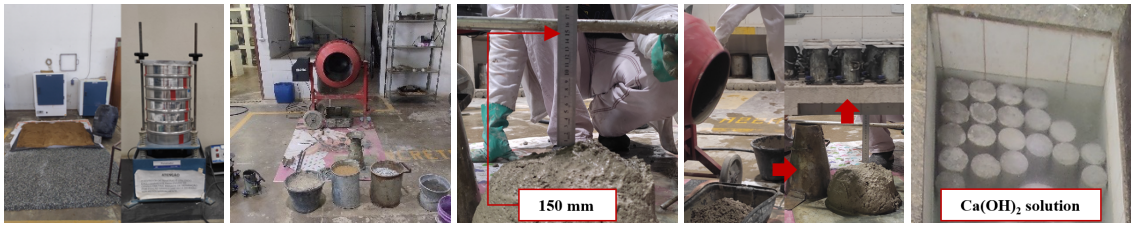

(a) (b) (c) (d) (e)

Fig. 2. Overview of concrete specimen production: (a) aggregates characterization; (b) mixing; (c) slump test; (d) casting; (e) curing after de-molding.

2.4. Experimental tests

2.4.1. Compressive strength

The compressive strength (f_c or *CS*) was determined at 28 days according to ABNT NBR 5739 [43]. A Universal Testing Machine (UTM)—EMIC PC Series hydraulic press, PC 200 CS Model, 2000 kN capacity—was used to compressively load the specimen toward its height (Fig. 3a) until it reached the maximum force (F) in Newtons. The outcomes were registered utilizing the TestScript software, being therefore possible to calculate the f_c through Eq. (1), where d is the specimen diameter in mm.

$$f_c = \frac{4 \cdot F}{\pi \cdot d^2} \tag{1}$$

(a) (b)

Fig. 3. Test setup: (a) compressive strength; (b) splitting tensile strength.

2.4.2. Tensile strength

The splitting tensile strength by diametral compression ($f_{ct,sp}$ or *TS*) was measured following ABNT NBR 7222 [44], also being carried out in the UTM—EMIC DL 30000 Model (Fig. 3b). The maximum force (F) was recorded in Newtons. Therefore, the $f_{ct,sp}$ was calculated through Eq. (2), where L is the specimen length in mm.

$$f_{ct,sp} = \frac{2 \cdot F}{\pi \cdot d \cdot L} \tag{2}$$

2.4.3. Static and dynamic modulus of elasticity

The static modulus of elasticity test was performed according to ABNT NBR 8522-1 [45], already knowing the specimen's compressive strength. An electronic strain gauge—EMIC EE Series, EEDA Model, 2.5 mm measuring range—was attached to the UTM (Fig. 4a) and then the following steps were employed: (i) centering the specimen in the lower plate, observing the molding direction; (ii) applying the loading at a constant speed of 0.45±0.15 MPa/s to the upper limit stress (σ_b = 0.3f_c) and holding for 60 s; (iii) unloading the specimen at the same speed to near zero stress; (iv) loading the specimen to the basic stress (σ_a = 0.5 MPa) and holding for 60 s; (v) loading the specimen to σ_b and holding for 60 s; (vi) unloading the specimen to near zero stress; (vii) repeating steps iv-vi; (viii) loading the specimen to σ_a, holding for 60 s, and recording the read strains (ε_a) in no more than 30 s; (ix) loading the specimen to σ_b, holding for 60 s, and recording the read strains (ε_b) in no more than 30 s; (x) calculating the static modulus of elasticity (E_s) by Eq. (3).

$$E_s = \frac{\sigma_b - \sigma_a}{\varepsilon_b - \varepsilon_a} \tag{3}$$

The Forced Resonant Frequency method assessed the dynamic modulus of elasticity (E_d). The experiments were conducted utilizing the Erudite MKII Resonance Frequency Test System by C.N.S. Electronics (Fig. 4b), adhering to the principles outlined in ASTM C215-08 [46] and BS 1881: Part 209 [47]. After obtaining the resonant frequency (f_r) in Hz, along with the specimen's diameter (d) and length (L) in meters, as well as its mass (m) in kilograms, the E_d in GPa is calculated. This calculation uses Eq. (4), designed explicitly for cylindrical specimens.

$$E_d = 5.093 \cdot \frac{L}{d^2} \cdot m \cdot f_r \cdot 10^{-3} \tag{4}$$

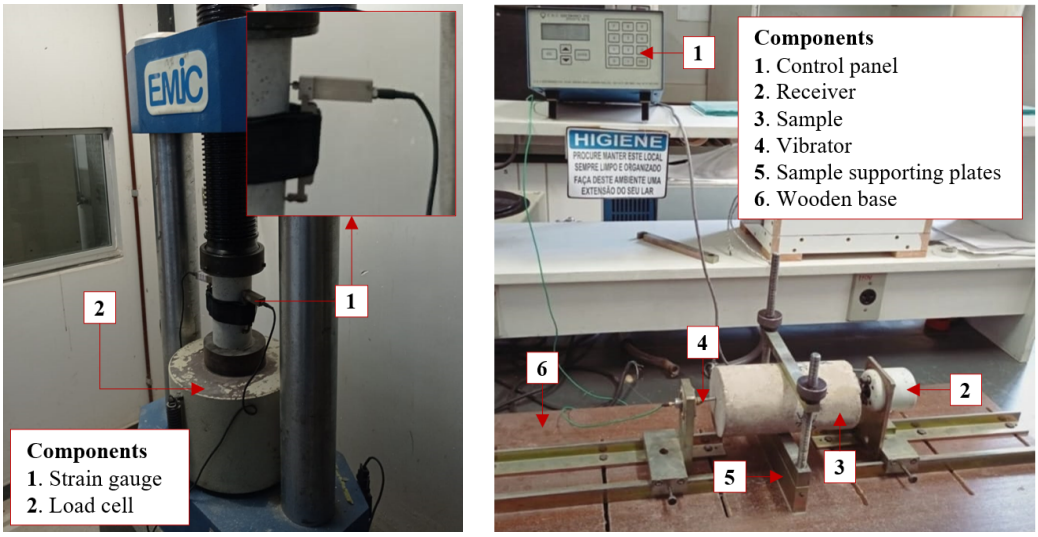

(a) (b)

Fig. 4. Test setup: (a) static modulus of elasticity; (b) dynamic modulus of elasticity.

2.4.4. Water absorption, porosity and bulk density

The water absorption, porosity, and bulk density tests were performed according to ABNT NBR 9778 version 2 [48]. The following steps were adopted: (i) drying the specimen in an oven at 100±5 °C for 72 h; (ii) determining the dry sample mass (m_d) using a weighing balance; (iii) immersing the sample in water at 23±2 °C for 72 h; (iv) measuring the saturated mass immersed in water (m_i) using a hydrostatic balance; (v) removing the sample from the water and drying its surface; (vi) measuring the saturated sample mass (m_{sat}); (vi) calculating the water absorption ($A_{(\%)}$ or WA), porosity ($P_{(\%)}$ or P), and bulk density (ρ_{ap}) using Eq. (5), Eq. (6), and Eq. (7), in this order. The ρ_{ap} considers the density of water (ρ) as 1 g/cm^3.

$$A_{(\%)} = \frac{m_{sat} - m_d}{m_d} \cdot 100 \tag{5}$$

$$P_{(\%)} = \frac{m_{sat} - m_d}{m_{sat} - m_i} \cdot 100 \tag{6}$$

$$\rho_{ap} = \frac{m_d}{m_d - m_i} \cdot \rho \tag{7}$$

2.4.5. Weight loss

The concrete's weight loss ($WL_{(\%)}$ or WL) was measured by sulfuric acid (H_2SO_4) attack. It is worth mentioning that although several works on concrete resistance to acid attacks have been developed [49], there are no standardized procedures for performing the tests, so techniques commonly used in scientific research were adopted. The steps followed were: (i) measuring the dry specimens' initial mass (m_1); (ii) immersing the specimens in a 5% solution H_2SO_4 bath, concentration employed by the literature [50–52]—the acid solution must be dropped into the water, not the water into the acid; (iii) removing the specimens at 7 days and brushing them slightly under running water until the color of the runoff, usually white, was reverted to clear water; (iv) drying the specimen in an oven at 100±5 °C for 72 h—CIENLAB oven, CE 220/150 Model, 150 L capacity; (v) recording the specimen's final mass (m_2); (vi) calculating the $WL_{(\%)}$ using Eq. (8).

$$WL_{(\%)} = \frac{m_1 - m_2}{m_1} \cdot 100 \tag{8}$$

2.4.6. Ultrasonic pulse velocity

The internal structure of the concrete was evaluated by the ultrasonic pulse velocity (*UPV*), whose test was performed with a sensor—Pundit Lab(+) Model made by PROCEQ. The test is based on the propagation of high-frequency sound waves through the material, whose velocity varies according to the number of voids and pores, which, in the case of cement-based composites, helps assess their uniformity or defects [53]. In Brazil, it is standardized by NBR 8802 [54].

Therefore, the concrete's quality can be assessed using *UPV*. When the *UPV* exceeds 4,500 m/s, the quality is considered "excellent". For values between 3,500 and 4,500 m/s, the classification is "good". The quality is considered "doubtful" between 3,000 and 3,500 m/s, while values between 2,000 and 3,000 m/s indicate "poor" quality. The quality is deemed "very poor" if the *UPV* is less than 2,000 m/s [55]. It is essential to highlight that this test, as it is non-destructive, plays a crucial role in evaluating the structural integrity of existing buildings.

2.4.7. Electrical resistivity

The electrical resistivity (*ER*) was measured using Wenner's method [56], which consists of applying an electric current to the two probes at the ends and then measuring the potential difference between the two inner probes. A 4–point Wenner probe—RESIPOD sensor, 38 mm Model, made by PROCEQ—was operated. Eq. (9) calculates the resistivity, where a is the distance between the electrodes, V is the voltage measured between the central electrodes and I is the current.

$$ER = \frac{2 \cdot \pi \cdot a \cdot V}{I} \tag{9}$$

This test evaluates the intensity of corrosion risk based on *ER*, mainly because it is non-destructive. The risk is considered very high when *ER* registers values below 50

Ω.m and high if the values are between 50 and 100 Ω.m. When the *ER* is 100 to 200 Ω.m, it is considered moderate to low; if the *ER* exceeds 200 Ω.m, the risk is low [57,58].

2.5. Statistical analysis

The Tukey means contrast test, conducted at a 5% significance level, assessed responses across varying CNT concentrations (0%, 0.05%, and 0.10%). In the context of Tukey's test, treatment groups were labeled alphabetically, with 'A' representing the one boasting the highest average property value, followed by 'B' for the second highest, and so on. Treatments sharing the same letter were deemed statistically comparable.

After examining CNT content influence, the correlation between the properties examined in this study (Pearson correlation: $-1 \leq r \leq 1$) was evaluated. Analysis of Variance (ANOVA) at a 5% significance level was employed to assess these correlations' significance. A *p-value* below 0.05 indicated a significant correlation, while values above 0.05 indicated non-significance.

After the correlation assessments, a quadratic regression model (Eq. (10)) was employed to estimate these properties. This regression type was chosen because the CNT effect may not be proportional to the increase in their content, and a linear model may not adequately represent variations in concrete properties. A quadratic model, however, allows the capture of curvatures in the relationship between CNT content and these properties and is more flexible in dealing with non-linear patterns.

$$Y = \beta_0 + \beta_1 \cdot CN + \beta_2 \cdot CN^2 + \varepsilon \tag{10}$$

In Eq. (10), Y represented the property to be estimated (dependent variable), CN (CNT content) was the independent variable, β_i denoted the model parameters adjusted using the least-squares method, and ε accounted for random error. The model's accuracy was assessed using the coefficient of determination (R^2—Eq. (11)). In this context, Y_{data_i} denoted the property's experimentally determined sample value, $\bar{Y}_{data_i}$ signified the average value derived from n experimentally determined sample values, and $Y_{predict_i}$ denoted the property value estimated by the regression model. Higher R^2 values, approaching 100%, signify better accuracy in the developed equation. However, it is worth noting that an R^2 greater than 70% (0.70) can still be considered an acceptable fitting level [59].

$$R^2 = 100 \cdot \left(1 - \frac{\sum_{i=1}^{n}(Y_{predict_i} - Y_{data_i})^2}{\sum_{i=1}^{n}(Y_{data_i} - \bar{Y}_{data_i})^2}\right) \tag{11}$$

Furthermore, the Anderson-Darling normality test (at a 5% significance level) was employed to validate the Tukey test results, regression models' ANOVA, and correlation tests. According to the test formulation, a *p-value* greater than or equal to the significance level implied a normal distribution assumption.

Based on the derived expressions, it is possible to estimate the concrete's physical and mechanical properties for CNT contents that fell outside the experimental design but within the 0% to 0.10% range. Despite specific authors proposed models for concrete behavior with carbon nanotubes [60,61], there needs to be more literature regarding models for estimating CNT–concrete's mechanical and durability properties.

3. Results and Discussion

3.1. Concrete properties

Fig. 5 presents the mean values, the coefficients of variation (CV), the means' confidence intervals (CI—95% reliability), the Tukey test's results (5% significance), and the Anderson-Darling (AD) test's outcomes (ANOVA validation—*p-value* ≥ 0.05) regarding the physical properties of the composites manufactured with 0% (reference), 0.05% and 0.10% CNT. Fig. 6, in turn, presents the results obtained from the mechanical and durability properties.

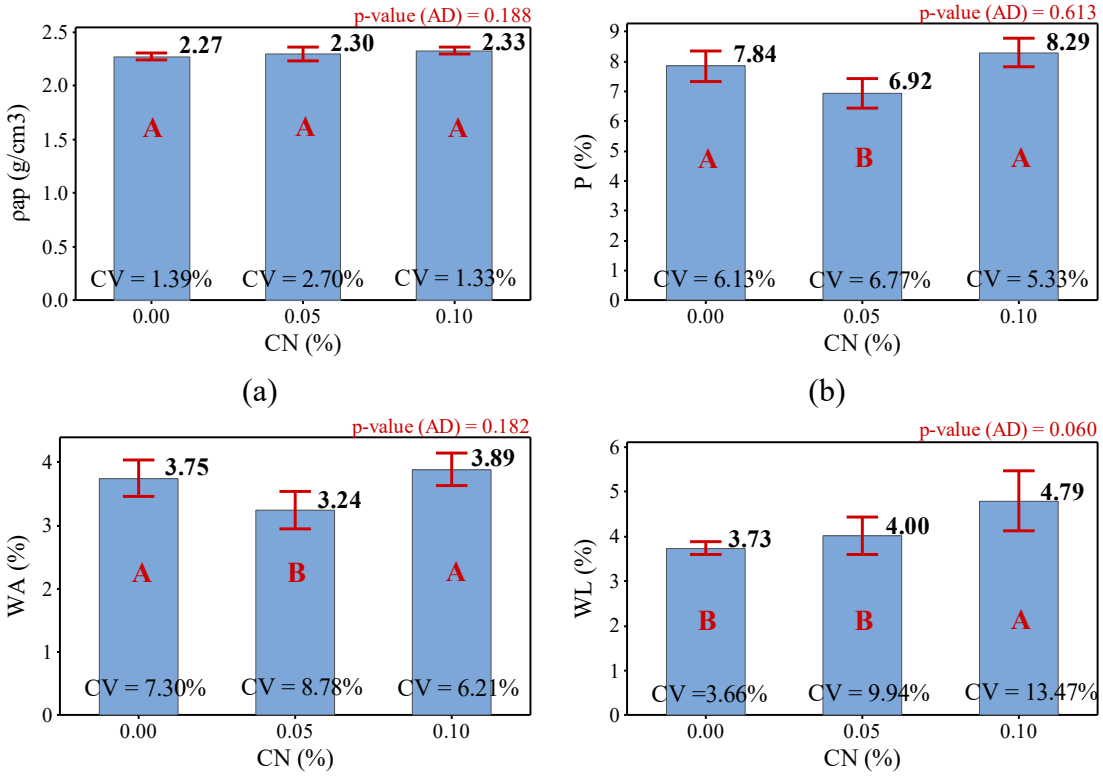

Fig. 5. Results of the physical properties of concrete with (0.05% and 0.10%) and without (reference) CNT: (a) ρ_{ap}—bulk density; (b) *P*—porosity; (c) *WA*—water absorption; (d) *WL*—weight loss.

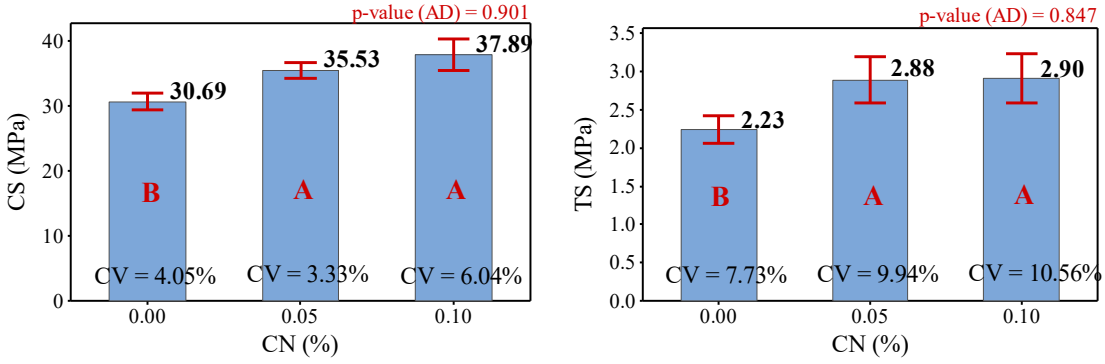

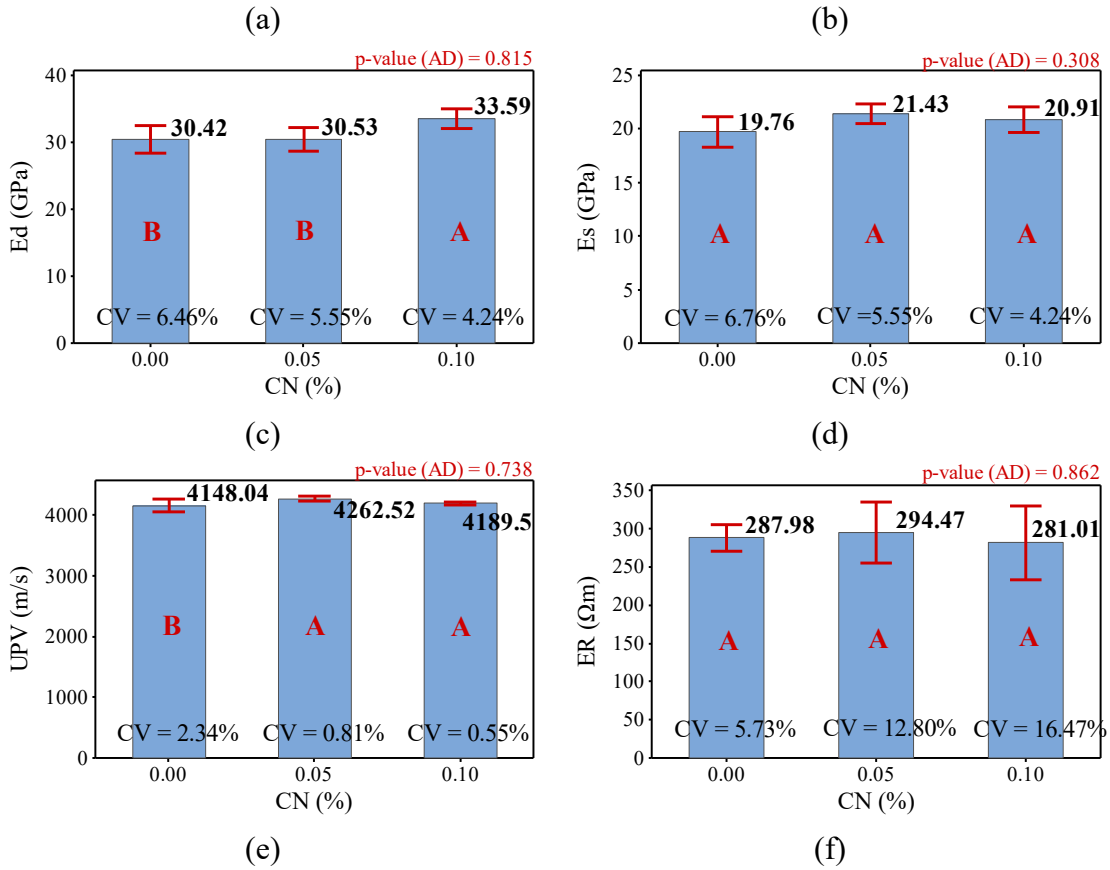

Fig. 6. Results of the mechanical and durability properties of concrete with (0.05% and 0.10%) and without (reference) CNT: (a) *CS*—compressive strength; (b) *TS*—tensile strength; (c) E_d—dynamic modulus of elasticity; (d) E_s—static modulus of elasticity; (e) *UPV*—ultrasonic pulse velocity; (f) *ER*—electrical resistivity.

The ρ_{ap} results (Fig. 5a) reveal that the reference sample ($CNT_{0.00}$) had a 2.27 g/cm^3 density, while $CNT_{0.05}$ and $CNT_{0.10}$ exhibited 2.30 and 2.33 g/cm^3 densities, respectively. However, the Tukey test indicated that these values' differences were insignificant. The increase in ρ_{ap} with the inclusion of CNT could not be statistically proven, suggesting that the CNT presence did not impact the ρ_{ap} relative to the control sample, which may be due to the possible non-uniform CNT dispersion or the relatively CNT low amount.

Fig. 5b shows that the *P* of $CNT_{0.00}$ was 7.84%, while $CNT_{0.05}$ showed a reduction to 6.92%, statistically differing from the other two samples. This decrease in *P* in $CNT_{0.05}$ can be attributed to the CNT action, which can fill some voids between the cement particles, resulting in a more compact structure. On the other hand, both $CNT_{0.00}$ and $CNT_{0.10}$ demonstrated statistically equal *P*. Comparing these two samples, *P* slightly increased in $CNT_{0.10}$, which may be due to CNT agglomeration, creating voids in the concrete matrix.

Regarding *WA* (Fig. 5c), $CNT_{0.00}$ had a 3.75% rate, while $CNT_{0.05}$ reduced to 3.24%, indicating a significant decrease due to CNT. This reduction is related to decreased *P*, which means fewer spaces are available for water to enter. On the contrary, $CNT_{0.10}$ showed increased *WA*, reaching 3.89%. This increase may be related to the increase in *P* in this sample.

Fig. 5d presents the results of *WL*, a property related to the concrete's ability to resist degradation caused by exposure to acidic substances, and the CNT incorporation can influence this resistance in several ways. The reference sample recorded a *WL* of

3.73%. In comparison, $CNT_{0.05}$ had a *WL* of 4%, with averages statistically equal to those of $CNT_{0.00}$, suggesting that adding 0.05% CNT did not significantly impact the concrete's resistance to acid attack. On the other hand, $CNT_{0.10}$ showed the highest *WL*, totaling 4.79%, and was statistically different from the others. However, $CNT_{0.10}$ showed a more substantial *WL*, indicating that a higher CNT content may make the concrete more susceptible to acid attack due to a greater concentration of reactive sites for the acidic action.

The results of the *CS* (Fig. 6a) and *TS* (Fig. 6b) are crucial indicators of the concrete's mechanical performance. $CNT_{0.00}$ had a *CS* of 30.69 MPa. In contrast, $CNT_{0.05}$ increased, reaching 35.53 MPa, and $CNT_{0.10}$ showed even greater strength, reaching 37.89 MPa. Statistical tests revealed that the means of $CNT_{0.05}$ and $CNT_{0.10}$ were higher than the reference sample but equivalent, indicating that 0.05% CNT may be sufficient for significant improvements in *CS*. Regarding *TS*, $CNT_{0.00}$ obtained 2.23 MPa, $CNT_{0.05}$ increased to 2.88 MPa, and $CNT_{0.10}$ reached 2.90 MPa. These results highlight the positive impact of incorporating CNT on concrete's *CS* and *TS*, attributed to the CNT's ability to reinforce the cement matrix and act as a bridge in the transfer of tensile stresses, with 0.05% CNT being enough to improve these properties substantially. It is worth mentioning that the *TS* measured by the diametral compression test is susceptible to variability due to the complex nature of the loading and the sample's geometric characteristics. The heterogeneous distribution of stresses along the rupture plane can lead to varying results between samples, even when manufactured under similar conditions, hence the high CVs in Fig. 6b.

The outcomes of E_d (Fig. 6c) and E_s (Fig. 6d) help to understand the concrete's ability to absorb and dissipate energy at different loading conditions. Concerning E_d, $CNT_{0.00}$ presented a value of 30.42 GPa. $CNT_{0.05}$ registered 30.53 GPa, slightly higher, and $CNT_{0.10}$ achieved a significantly higher E_d of 33.59 GPa. Notably, $CNT_{0.00}$ and $CNT_{0.05}$ had means statistically equal, indicating that 0.05% CNT did not significantly affect the E_d. Regarding the E_s, values of 19.76 GPa, 21.43 GPa, and 20.91 GPa were obtained for $CNT_{0.00}$, $CNT_{0.05}$, and $CNT_{0.10}$, respectively, with statistical equivalence. These outcomes suggest that adding CNT had a limited influence on the concrete stiffness under static loading, which follows the literature [62]. It is worth noting that although the tests to measure E_s are destructive and those to measure E_d are non-destructive, the differences between these modules are generally minor, considering the adequate sample's dimensions and the CNT's effects.

UPV testing, in turn, is a valuable tool for inspecting and evaluating concrete structures, helping to identify areas of concern and guiding decision-making regarding maintenance, repair, or replacement of concrete components in various applications, from construction to infrastructure. As evidenced in Fig. 6e, the control sample recorded a *UPV* of 4148 m/s, $CNT_{0.05}$ reached 4262 m/s, and $CNT_{0.10}$ obtained 4189 m/s. Statistically, the CNT–concrete samples had equivalent means but were significantly higher than the reference. This increase in *UPV* suggests more significant densification or cohesion in the concrete's matrix due to the CNT presence. Furthermore, the similarity of $CNT_{0.05}$ and $CNT_{0.10}$ mean values suggests that 0.05% CNT may have already achieved a maximum effect in improving the *UPV*, indicating that it is not necessary to increase the CNT content to obtain substantial improvements in the ultrasonic wave propagation in concrete. Besides, CNT–concrete samples presented *UPV* in the "optimal quality" range (3500–4500 m/s), suggesting that, based on available data and the standard rating, incorporating CNT did not lead to the concrete achieving the "excellent" quality rating in terms of *UPV*. However, this does not necessarily mean that adding CNT does not benefit other concrete's properties or application conditions, as several factors, including the

concrete's age, the aggregate type, humidity, temperature, and the additives' presence, can influence *UPV* values.

The results of *ER* (Fig. 6f) indicate that adding CNT to concrete did not impact the material's ability to conduct electricity. $CNT_{0.00}$, $CNT_{0.05}$, and $CNT_{0.10}$ samples showed similar *ER* values, 288 Ω.m, 294 Ω.m, and 281 Ω.m, respectively. However, it is essential to note that the CVs of the CNT–concrete samples were relatively high, indicating considerable variability in the outcomes. Therefore, based on available data, incorporating CNT does not significantly affect the concrete's *ER*.

3.2. Effectiveness of dispersion techniques

Before discussing the reasons for improving or worsening the properties studied here, considering the use of CNT pre-dispersed in cement particles in an isopropanol medium, it is worth comparing these variations with those documented in the existing literature, shown in Fig. 7 (*CS* compared to refs. [18,20,22–24,63–66]), Fig. 8 (*TS* compared to refs. [20,22–24,64,66,67]), Fig. 9 (*P* compared to refs. [68,69]), and Fig. 10 (*UPV* compared to refs. [20,65,70]). In these figures, "PF" signifies the use of CNT in powder form, and "AS" denotes their utilization in an aqueous suspension. The term "NS" is used when the specific form of the CNT is not detailed in the paper. Additionally, "LWGC" stands for lightweight geopolymer concrete and "UHPC" represents ultra-high-performance concrete. The numbers in blue or red indicate the percentage variation in the property of that sample about the reference concrete.

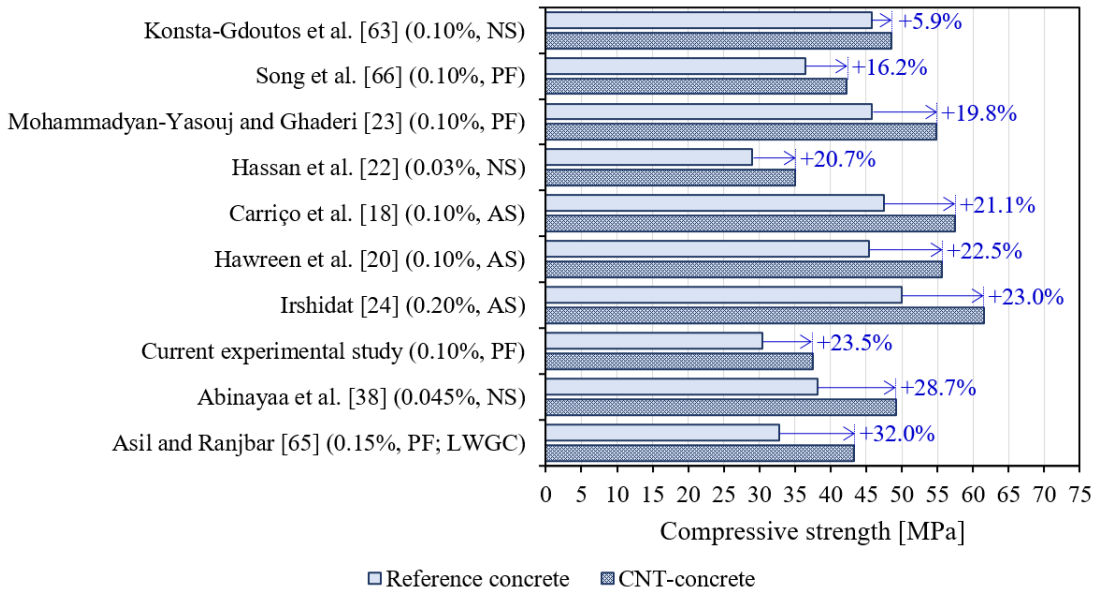

Fig. 7. Compressive strength: Comparison of experimental results with literature.

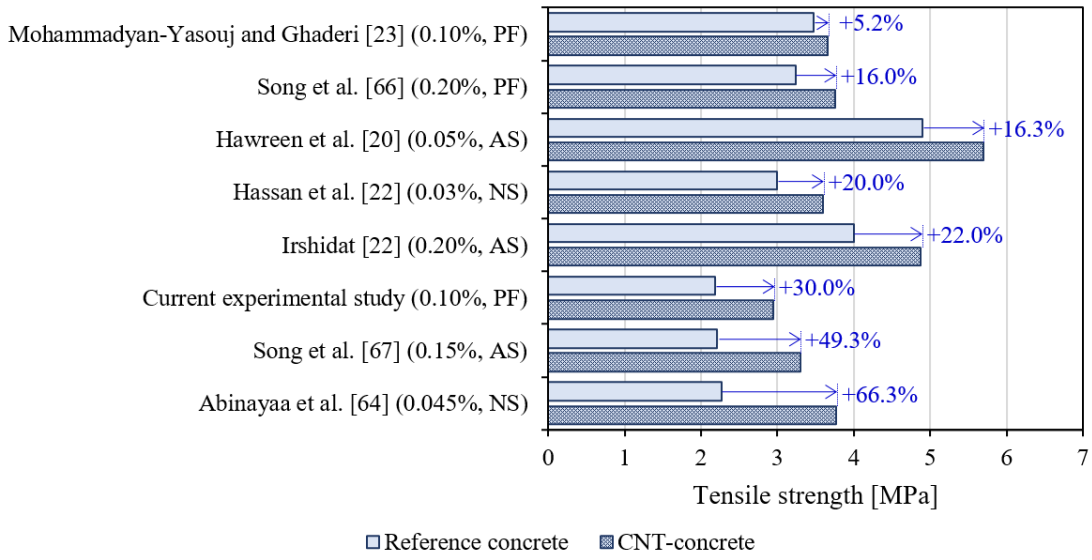

Fig. 8. Tensile strength: Comparison of experimental outcomes with literature.

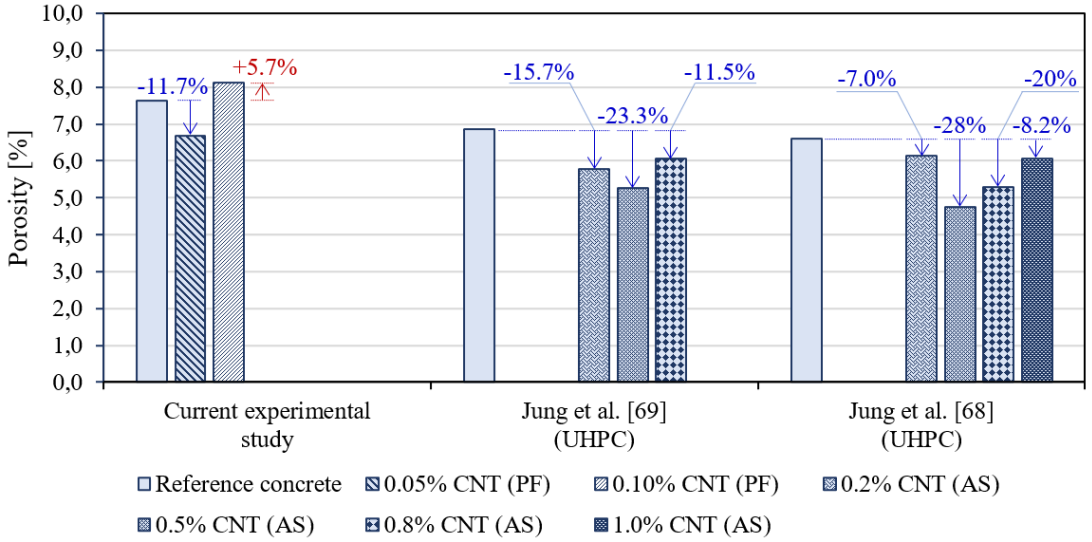

Fig. 9. Porosity: Comparison of experimental data with literature.

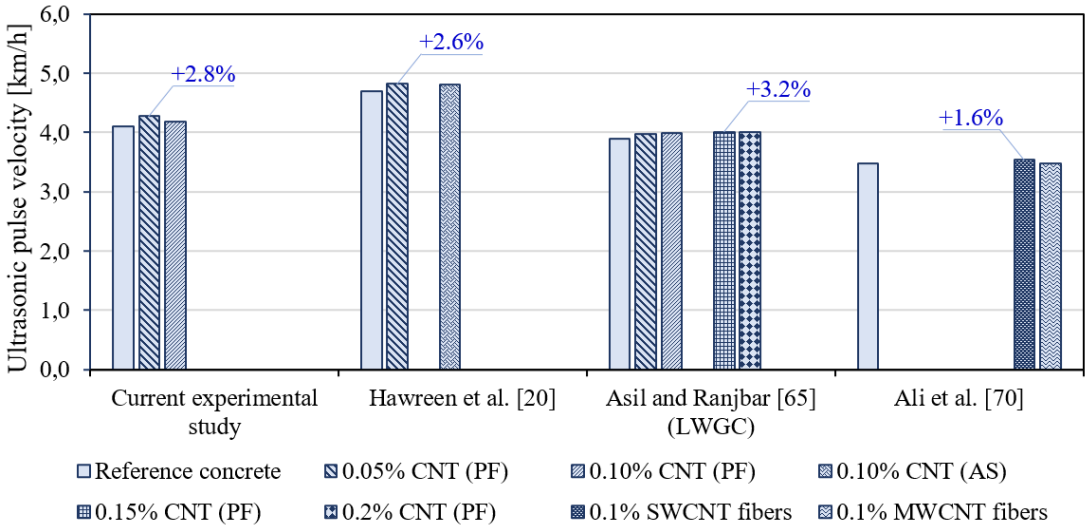

Fig. 10. Ultrasonic pulse velocity: Comparison of experimental results with literature.

Fig. 7 shows that adding CNT increased the *CS* in all samples studied, with improvements ranging from +5.9% to +32.0% about the reference concrete. It was observed that the CNT form, whether in powder or aqueous suspension and the CNT content influence the performance of concrete. The current experimental study showed an increase of +23.5% with 0.10% CNT in powder form, aligning with similar results in the literature.

Improvements in *TS* were also evident with the inclusion of CNT, with increases from +5.2% to +66.3%, as seen in Fig. 8. Again, the CNT concentration and form varied. However, there was no direct correlation between the CNT content and the increase in strength. The current experimental study recorded a significant increase of +30.0%, presenting evidence that the pre-dispersion of CNT in cement may be effective in improving the *TS* of concrete.

Fig. 9, in turn, depicts that using CNT variedly influenced *P*. While some mixtures showed a significant reduction, such as -23.3% and -28.0%, the current study showed assorted results, with a -11.7% reduction in samples with 0.05% CNT and an increase of +5.7% with 0.10% CNT, both in powder form. This fact suggests that the efficiency in reducing *P* depends on the CNT dispersion method and that there may be a concentration limit of CNT so that there are no undesirable results. It is important to note that only some studies on concrete with CNT explain porosity measurements, so research with UHPC was selected.

Finally, all concrete modified with CNT in powder form and aqueous suspension, or CNT fibers, exhibited an increase in *UPV*, which suggests an overall improvement in concrete quality. The greater increases ranged from +1.6% to +3.2%, with the current study showing a *UPV* one of +2.8% with the addition of 0.05% CNT, as indicated in Fig. 10. These results reinforce the perception that CNT have the potential to make concrete more homogeneous and with better mechanical properties. It should be mentioned that few works used *UPV* in studies involving concrete with CNT, which is why one that used a different concrete (LWGC) and another that used CNT fibers were selected for this comparison.

The analysis of the results proved the effectiveness of pre-dispersion of CNT in cement particles in an isopropanol medium. In terms of *CS*, this dispersion technique led to a performance equivalent to research using other methods to disperse CNT in aqueous suspensions, such as Carriço et al. [18] (+21.1% using sonication for 45 min in 3 cycles of 15 min), Hawreen et al. [20] (+22.5% employing magnetic stirring in water with surfactant and sonication for 30-45 min), and Irshidat [24] (+23.0% through dispersion in water and manual agitation followed by sonication for 20 min). Considering *TS*, the results of the current study were better than those of the references above (+30.0% against +22.0%, maximum) but lower than what Song et al. [67] obtained when dispersing CNT in aqueous suspension using only mixing with water and sonication, a more straightforward method (+30.0% against +49.3%). Regarding *P* and *UPV*, pre-dispersing CNT in cement particles (current study) was only practical for the 0.05% CNT content. However, studies using CNT in aqueous suspension had equivalent or even better results, even at higher concentrations.

From this perspective, dispersing CNT in aqueous suspension is generally simpler, safer and potentially more effective than the powdered form. Although there are effective dispersion techniques for powders, such as the pre-dispersion of CNT in cement particles using isopropanol (used in this study), they perform satisfactorily on a laboratory scale. However, they may face limitations when applied industrially, as highlighted by Son et al. [71].

In addition, Song et al. [66] observed that using industrial-grade CNT in aqueous suspension resulted in significant increases in concrete strength and deformation, particularly in the first seven days, a critical period for the appearance of cracks due to shrinkage and hydration heat. This finding suggests that the dispersion of CNT in an aqueous suspension may be more efficient in preventing cracks in young concrete and require fewer tests when compared to the use of fine nanotube powders.

Therefore, choosing CNT in aqueous suspension with industrial dispersion proves to be a more practical and safer approach for applying CNT in concrete. This fact corroborates the statement by Marcondes and Medeiros [16], who point out that the industrial dispersion process is remarkably superior to the alternatives tested in the laboratory.

3.1.1. Overall analysis and future perspectives

Adding CNT to concrete exhibited distinct effects on its properties. On the one hand, 0.05% CNT positively reduced *P* and *WA*, indicating an improvement in resistance to the penetration of aggressive agents, such as water and chloride ions. However, 0.10% CNT resulted in less favorable results, indicating a possible limit to the amount of CNT to be incorporated before its effect becomes counterproductive. Furthermore, it was observed that the CNT provided notable improvements in concrete's *CS* and *TS*, with 0.05% CNT being considered effective in obtaining these improvements without increasing the content to 0.10% CNT, which could result in additional costs without substantial additional benefits.

In this scenario, it is pertinent to explore why the strength increased despite the increase in *P* when incorporating 0.10% CNT into concrete. Firstly, more than *P* alone is needed to determine the concrete's strength since it is influenced by the number of pores and their size and distribution. Furthermore, the CNT presence in the sample at 0.10% ($CNT_{0.10}$) may have acted as reinforcement in the cement matrix, preventing the displacement of cracks and microcracks and contributing to a significant increase in *CS* and *TS*. Some research has been carried out in this direction.

Pores significantly impact the materials' macroscopic characteristics, such as deformation, strength, and durability [72,73]. In the case of concrete, a typical porous material, the pore distribution varies in shape and size, from microscopic to macroscopic [74], and their characteristics are linked to these pores' morphology, distribution, and other factors in addition to porosity [75]. Thus, modifying materials to achieve specific physical characteristics mainly involves reducing the total volume of physical pores and increasing the microscopic pore distribution [76].

In this sense, some authors carried out a microstructural analysis by scanning electron microscopy (SEM) and X-ray diffraction (XRD) and revealed the formation of the crystalline structure of calcium silicate hydrates (C–S–H) and calcium hydroxide (CH) gels, indicating that a denser microstructure was obtained in the concrete after adding nanosilica (NS) and CNT. They reported that the mixture with 0.5% NS and 0.04% CNT performed better than the others [77]. Another study indicated that the CNT incorporation increased the content of prismatically hexagonal CH, the proportions of gel pores, and harmless capillaries, as well as reduced the concrete's *P*, resulting in improved dynamic *CS* [78]. The impact of MWCNT on the mechanical properties and microstructure of reactive powder concrete (RPC) in dry-wet cycles with a high sulfate concentration was also investigated. SEM and XRD were used to analyze the RPC's microstructure and phase composition, and X-ray computed tomography to evaluate its internal pores and *P*. The test results indicated that the nanomaterials filled pores and

cracks and created bridges between cracks, reinforcing the RPC's resistance to sulfate attack [79].

As reported in many research, as the concrete's *P* increases, its strength tends to decrease. In this sense, adding CNT can have a positive effect up to certain limits. Jung et al. [80] studied the CNT's influence on the pore distribution in ultra-high performance concrete (UHPC) and the change in the volume of each pore type classified based on pore diameter at different CNT contents. The pore structure of UHPC changed dramatically as the amount of CNT incorporated varied, with a significant reduction in micropores (< 4.5 nm) and mesopores (4.5–25 nm) in almost all samples due to physical filling with CNT of similar sizes. However, the mesopores increased slightly when 0.8% CNT was added, suggesting that individual CNT effectively fill the nanopores in the C–S–H gel at lower concentrations, but at higher concentrations, van der Waals forces lead the CNT to form agglomerates, increasing the size and volume of the capillary pores [80]. These authors also reported that the trapped air voids formed at 100–25 μm increased at all contents, but especially at the higher ones, although the total *P* was still lower than that of the reference sample. Although the present research is not with UHPC, these findings help try to understand the relationship between porosity and strength previously mentioned.

The results regarding E_d and E_s, in turn, indicated that the CNT addition can improve the concrete's ability to resist dynamic loads without compromising its stability under static loading, which may be relevant in several civil engineering applications. However, the highest E_d occurred in the most porous sample, which draws attention. The relationship between these two properties is also complex in concrete, and the increase in E_d in the $CNT_{0.10}$, despite a slight increase in *P*, can be influenced by other factors. As in the discussions about *CS*, possible reasons are the pore size and distribution and the CNT's effect, which may act as reinforcements at the interfaces between cement particles and aggregates, improving the material's cohesion and stiffness under dynamic loading.

Regarding *WL*, adding 0.05% CNT did not significantly impact the concrete's resistance to acid attack, which is good news as other properties, such as *CS* and *P*, improved in this regard. The 0.10% CNT content had an adverse effect, increasing the *WL* due to acid attack. These results are consistent with those obtained in the RPC after exposure to a sulfate dry-wet cycling environment (10% Na_2SO_4 solution), with non-important reductions in *WL* in the control sample and a modest increase when 0.10% MWCNT was incorporated into the mixture [79].

It is worth noting that the degradation process occurs very slowly and can take years before corrosion is observed [81]. Therefore, accelerated *WL* tests, with a high acid concentration and a short exposure period, simulate concrete exposure to severe environments. H_2SO_4, in particular, is responsible for concrete deterioration, attacking the cement matrix and causing corrosion and, consequently, leading to a loss of strength and cohesion in the calcium compounds present in the mix [82]. These additional mechanisms highlight the complexity of acid attack on concrete and the importance of carefully evaluating its properties under different conditions and with additives such as CNT.

Concerning the *UPV* results, there was an improvement in the CNT–concrete samples, indicating that the CNT may contribute to greater cohesion and densification in the concrete matrix. Notably, 0.05% CNT has proven effective in increasing *UPV*, while there is no evidence that 0.10% CNT provides a more significant benefit. According to existing research, a significant connection exists between *UPV* and *P* and the concrete components' integrity [83]. When the ultrasonic wave encounters higher resistance, this generally suggests the presence of more porous structures and an interfacial transition zone (ITZ) with lower resistance, as highlighted in previous studies [84,85]. Moreover,

some authors have associated the rise in *UPV* values with the CNT's influence, contributing to an expansion of the C–S–H gel volume [70]. Therefore, the outcomes of the present study indicate that adding an adequate amount of CNT can improve the concrete's quality in this aspect, the *UPV* being a relevant metric for detecting defects and evaluating structural integrity.

Furthermore, the results reveal that adding CNT had a minimal effect on the concrete's *ER*, contrary to initial expectations. Given the CNT's low density and high aspect ratio, their inclusion would increase the samples' electrical conductivity. However, the outcomes indicate that, at the amounts tested, CNT did not adversely affect the concrete's ability to resist the flow of electrical current. Some authors reported a slight effect of the CNT on the UHPC's *ER* when contents of up to 0.80% CNT were used, and for 0.02% and 0.05% CNT, there was almost no change. Above 0.80% CNT, there was an increase in electrical conductivity [68,69]. Another study indicated that the UHPC's *ER* decreased modestly as the CNT content increased [86]. For these cases, it should be noted that the dosage of UHPC is generally different from ordinary concrete, with a lower w/c ratio and using other additions, such as fumed silica or silica powder. In addition, the literature has reported that 0.10% CNT was the content with the best results in the concrete's *ER* [19]. Nevertheless, it should be emphasized that none of these studies presented statistical analyses to affirm whether these improvements in the concrete's electrical properties were, in fact, significant, their results concerning only the relative differences between the average values.

Finally, it is worth highlighting that all the results discussed above are directly related to the w/c ratio used in the mixtures. A lower w/c could eventually allow CNT to exert a more pronounced impact on concrete's properties, especially in decreasing porosity and pore size. However, this decision must consider the project's specific requirements and the practical feasibility of mixing and curing the concrete, as did this research.

These complex interactions between w/c ratio, porosity, strength, CNT, and other concrete components, as well as the dispersion techniques, highlight the need for detailed analyses to fully understand the effects of several CNT contents and optimize their use in concrete. Although the results suggest that CNT incorporation may be a promising strategy for improving the concrete's mechanical performance, especially in applications such as construction, they draw attention to the critical importance of accurately adjusting the CNT content to avoid undesirable effects on other concrete's properties. Therefore, continued research is crucial to understanding the effects of different CNT contents, how they affect concrete's properties under different mixing and curing conditions, and their durability in varying environments.

3.3. Correlation between properties

The results of the correlation analyses (Pearson correlation: $-1 \leq r \leq 1$) for the composites manufactured without (Table 4) and with 0.05% (Table 5) and 0.10% CNT (Table 6), respectively, are presented below, with the underlined correlations being considered significant by ANOVA (*p-value* < 0.05). Such correlations were evaluated to verify the existence of a significant relationship between the response variables considered and whether the CNT inclusion preserves the correlations obtained from the reference condition.

Table 4. Correlations tested for $CNT_{0.00}$ samples (reference).

Var.	ρ_{ap}	*P*	*WA*	*WL*	*CS*	*TS*	E_d	E_s	*UPV*

P	-0.331								
WA	-0.491	0.984							
WL	-0.692	0.359	0.459						
CS	0.559	-0.582	-0.636	-0.257					
TS	-0.954	0.396	0.543	0.863	-0.451				
E_d	0.405	0.050	-0.027	0.331	0.587	-0.129			
E_s	0.370	0.354	0.255	-0.629	-0.480	-0.508	-0.426		
UPV	0.665	-0.532	-0.619	-0.416	0.125	-0.686	0.108	0.287	
ER	0.550	0.019	-0.082	0.031	0.728	-0.305	0.880	-0.275	-0.030

Table 5. Correlations tested for $CNT_{0.05}$ samples.

Var.	ρ_{ap}	***P***	***WA***	***WL***	***CS***	***TS***	E_d	E_s	***UPV***
P	-0.412								
WA	-0.673	0.951							
WL	-0.259	0.263	0.292						
CS	0.073	-0.755	-0.634	-0.617					
TS	0.251	-0.090	-0.147	-0.854	0.535				
E_d	0.011	0.330	0.267	-0.344	0.209	0.652			
E_s	0.472	-0.134	-0.279	0.417	-0.447	-0.678	-0.576		
UPV	-0.676	-0.034	0.207	0.276	0.098	-0.145	-0.311	-0.509	
ER	-0.118	-0.675	-0.515	0.368	0.312	-0.616	-0.665	0.392	0.296

Table 6. Correlations tested for $CNT_{0.10}$ samples.

Var.	ρ_{ap}	***P***	***WA***	***WL***	***CS***	***TS***	E_d	E_s	***UPV***
P	-0.154								
WA	-0.370	0.975							
WL	0.405	-0.166	-0.245						
CS	0.323	0.111	0.032	-0.163					
TS	-0.188	0.494	0.509	-0.616	0.547				
E_d	-0.226	-0.312	-0.242	0.094	-0.937	-0.439			
E_s	0.493	-0.305	-0.398	0.745	0.206	-0.672	-0.321		
UPV	0.837	-0.133	-0.314	0.734	0.164	-0.557	-0.224	0.850	
ER	-0.206	-0.566	-0.490	-0.528	-0.247	-0.297	0.304	-0.128	-0.274

A significant correlation occurred between *P* and *WA* in all samples, i.e., such properties are intrinsically linked, and including CNT, regardless of the content, did not affect this relationship. This outcome is intuitive in physical terms, as *P* acts as a network of channels for water to flow and be stored in the material. Thus, any change in *P*, whether due to additions such as CNT or other factors, can influence *WA*, but the fundamental association between these properties remains consistent.

Furthermore, it was noted that higher *WL* is associated with lower *TS*, indicating a potential weakening of the concrete due to degradation. This effect was consistent in $CNT_{0.00}$ and $CNT_{0.05}$. However, this correlation was no longer significant in the $CNT_{0.10}$, suggesting that there may be a saturation point where the additional amount of CNT no longer contributes significantly to the relationship between *WL* and *TS*. Once this point is reached, increasing the CNT content may not have a discernible additional impact.

Still talking about *TS*, this property only significantly correlated with the ρ_{ap} in the reference sample. As the ρ_{ap} of all samples is equivalent (with or without CNT), it can be inferred that the CNT presence or amount does not influence the initially observed correlation between ρ_{ap} and *TS*. In other words, the consistency in ρ_{ap} indicates that the variation in *TS* should be attributed to factors other than ρ_{ap} or CNT. Similar logic can be used to discuss the significant correlation between ρ_{ap} and *UPV* in the $CNT_{0.10}$, which may have been influenced by the CNT's intrinsic characteristics or by variations in the microstructural properties of the concrete matrix related to the CNT. Regardless of ρ_{ap}, these factors may affect how ultrasonic waves propagate in concrete samples.

Finally, the analysis of the outcomes revealed interesting patterns regarding the other mechanical properties. In $CNT_{0.00}$, a correlation was observed between the E_d and E_s, suggesting a relationship between them. However, it is essential to consider that these moduli can be affected by frequency tests and loading conditions. In $CNT_{0.10}$, a significant correlation was observed between the *CS* and E_d, indicating that this content positively influenced both in this case, which did not occur with $CNT_{0.05}$ samples, with no significant correlation identified between the E_d and E_s, neither between *CS* and E_d nor between E_d and E_s.

The lack of significant correlations between some concrete's properties can be due to its complexity as a composite material, subject to the influence of several factors. For example, the results may partially arise from the intricate interactions between carbon nanotubes and the concrete's matrix, indicating that CNT can potentially modify the relationships between different concrete's properties. Furthermore, the multifaceted behavior of concrete makes correlations sensitive to several variables.

It is crucial to emphasize that choosing samples with similar sizes was made deliberately to ensure more reliable results. The limit of five specimens was determined by the properties measured in the destructive tests. This consideration is particularly relevant since non-destructive testing was conducted on all the samples intended for destructive testing, resulting in a more comprehensive database for physical properties (greater than five). In other words, the correlation of the results and the durability properties (obtained non-destructively) could have been improved if the samples had not been chosen randomly, as we did to maintain integrity, but rather selected based on more notable values.

It is also worth highlighting that carrying out experiments to find the optimal CNT content without considering the correlations between properties can be costly and time-consuming. However, based on correlations, reducing the number of tests required is possible, saving resources. Correlations can also guide concrete mix optimization, allowing for a more targeted approach. By understanding how different CNT amounts affect concrete's properties, it is feasible to perform regression analyses, such as quadratic, to determine the optimal CNT content that will lead to specific property improvements, making developing new concrete materials more efficient.

3.4. Quadratic regression models

In order to verify the existence of optimal CNT contents (between 0% and 0.10%) in the investigated properties, quadratic regression models evaluated by ANOVA (5% significance) were considered. Table 7 presents the regression models considered significant by ANOVA (*p-value* < 0.05), the determination coefficients (R^2), and the respective nanotube content (CN^{opt}) that make the response values extreme, making it possible to investigate whether it is feasible to obtain properties equivalent to those

obtained with 0.10% but for a lower amount of this material, and Fig. 11 shows the fitted curves.

Table 7. Quadratic regression models considered significant by ANOVA.

Model	R^2 (%)	CN^{opt}	Max or Min
$P\ (\%) = 7.840 - 41.30 \cdot CN + 458 \cdot CN^2$	64.39	0.045	Minimize
$WA\ (\%) = 3.750 - 21.77 \cdot CN + 231.3 \cdot CN^2$	56.57	0.047	Minimize
$CS\ (MPa) = 30.69 + 121.4 \cdot CN - 494 \cdot CN^2$	79.77	0.123	
$TS\ (MPa) = 2.233 + 19.18 \cdot CN - 125 \cdot CN^2$	62.74	0.077	Maximize
$UPV\ (m/s) = 4148 + 4165 \cdot CN - 37502 \cdot CN^2$	41.06	0.056	Maximize

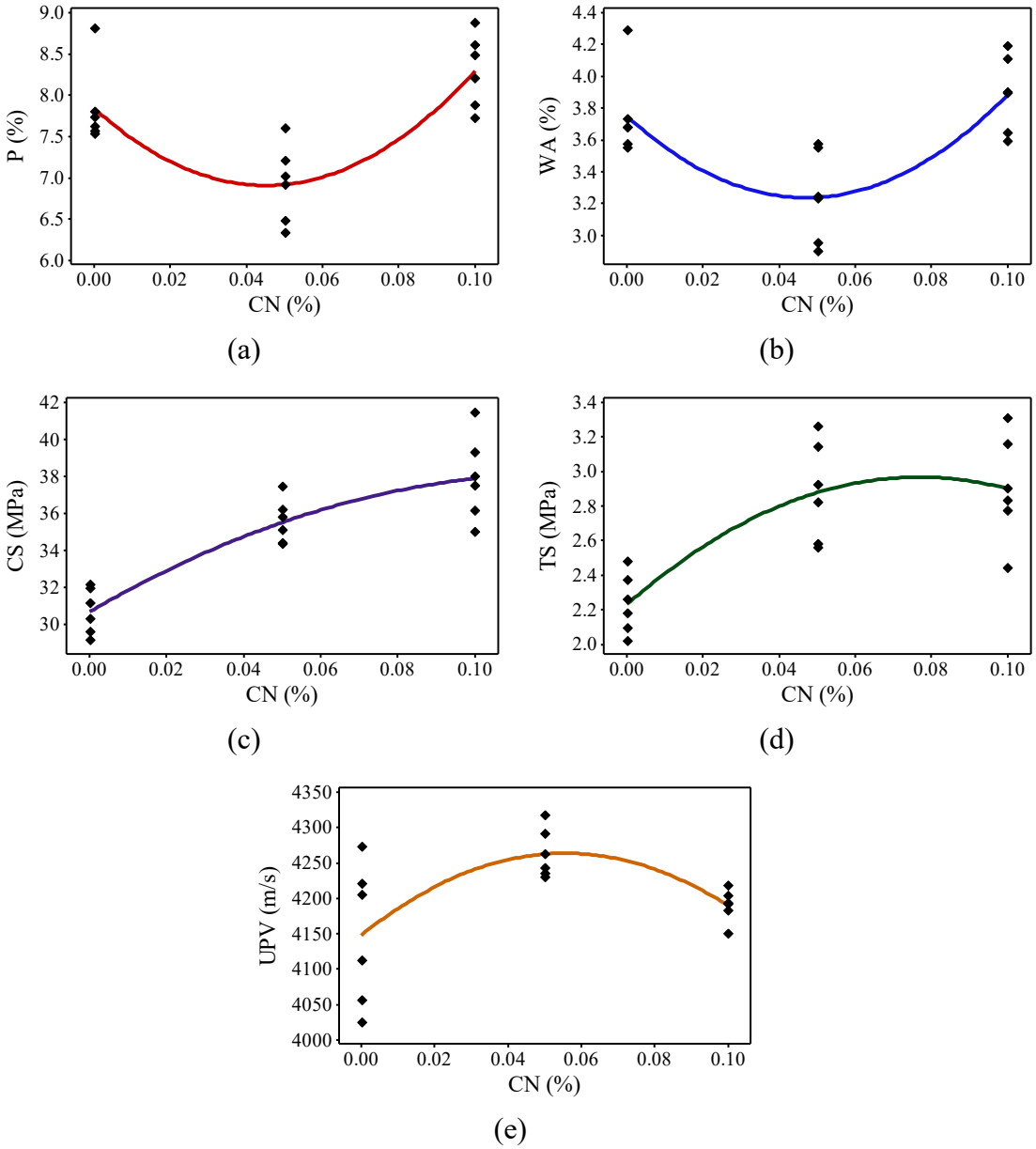

Fig. 11. Curves fitted to experimental data.

The regression models in Table 7 and Fig. 11 demonstrate quadratic relationships between concrete's properties and CNT content. The R^2 ranges from 41.06% to 79.77%, indicating that the model explains variability in properties, such as *P*, *WA*, *CS*, *TS*, and

UPV based on CNT concentration. CN^{opt} values range from 0.045% to 0.123%, suggesting specific CNT contents to optimize each property. This is relevant to improving the concrete's quality and durability, reducing *P* and *WA* while increasing *CS* and *TS*, depending on the application needs.

Finding a single CN^{opt} that best meets all properties simultaneously can be challenging, as different properties can have conflicting requirements. However, an intermediate CNT content can be achieved using a weighted average of the optimal concentrations, i.e., the R^2 values can be the weights (the higher the R^2, the greater the weight) for each property. This method may help determine the content that globally optimizes the CNT–concrete's performance concerning these properties.

It is important to note that although these quadratic regression models provide an initial estimate of CNT content that optimizes each property, these are theoretical outcomes based on relationships identified in existing data. For a practical application, additional experiments with a larger sample are welcome to increase the model's reliability, reduce variability in the data, and improve the fit of the models (increase R^2). In this case, it also helps confirm these results and evaluate other considerations, such as the cost and availability of CNT.

It is true that, based on the results of this study, the benefits of adding CNT to concrete were found to be modest in some properties, such as *CS* and *TS*, which follows the literature and is an important observation. For example, some authors reported an increase in concrete's *CS*, *TS*, and steel-concrete bond strengths. However, the advantages of using CNT were moderate. These authors also stated that other additions or mineral/chemical fibers could improve the concrete's mechanical properties without the problems associated with CNT dispersion and the health risks from handling a nanomaterial [22]. Another study considered the improvement of the concrete's mechanical properties with the CNT incorporation to be unattractive, at least considering the CNT dispersion method used and the high cost of CNT on the market to date [87]. Given this, why continue investigating the potential of CNT in cementitious materials, especially concrete?

Studies on using CNT in cementitious materials, mainly concrete, involve important concerns. Although the benefits may be moderate and the dispersion and cost challenges are real, the potential of CNT in cement-based materials applications remains. Research is evolving, and the development of improved dispersion methods and a deeper understanding of CNT–concrete interactions could lead to significant advances in the future. Furthermore, the choice between CNT and other materials depends on the project's specific needs and desired properties, as CNT stand out for their unique electrical conductivity and mechanical properties. Even though they are expensive, their nanometric characteristics can justify their use in high-performance applications. Continued research in nanotechnology can make CNT more accessible and practical in construction applications. Therefore, studies on including CNT in concrete are justified, as they are essential in high-performance applications and technological innovation, especially when seeking to improve concrete structures' bonding, strength, electrical conductivity, and durability.

Moreover, it is worth mentioning the fundamental role of statistical studies in predicting the physical and mechanical properties of cementitious materials by adding nanomaterials. Besides, the usefulness and importance of tests, especially non-destructive tests, such as *UPV* and *ER* ones, should be highlighted in the continuous search for significant advances and in optimizing CNT and other nanomaterials in civil construction applications.

4. Conclusions

This paper evaluated the concrete properties (ρ_{ap}, P, WA, WL, CS, TS, E_d, E_s, UPV, and ER) considering three CNT contents (0%, 0.05%, and 0.10%) and proposed regression models to estimate them. The following conclusions can be drawn:

i. The statistical analysis indicated significant reductions in P (up to 12%) and WA (up to 14%) and increases in CS (up to 16%), TS (up to 29%), and UPV (up to 3%) with 0.05% CNT. In addition, an improvement was observed in E_d (up to 10%) with 0.10% CNT, while WL significantly increased (up to 28%) with the same CNT content. No significant effects were observed on ER and E_s. These data suggest that optimizing the CNT amount requires detailed analysis to avoid undesirable effects.

ii. Considering the variations in CS, TS, P, and UPV obtained in this research and the literature, the pre-dispersing powdered CNT in cement particles using an isopropanol medium was effective for applications in concrete. However, the dispersion of CNT in aqueous suspension offers a simpler, safer, and potentially more efficient solution, particularly when considering applications on an industrial scale. This comparison highlights the need for effective methods in a laboratory setting that are scalable and practical for real-world construction scenarios.

iii. There were significant correlations between P and WA and a negative correlation between WL and TS, which became non-significant for 0.10% CNT, suggesting the existence of a CNT saturation point. In addition, there was a correlation between ρ_{ap} and UPV in the samples with 0.10% CNT and a positive influence of this content on the relationship between CS and E_d. A significant correlation between E_d and E_s occurred only in the reference sample. Therefore, it can be seen that a variation in any property causes changes in the others, hence the importance of further investigations on the correlation between physical and mechanical properties of concrete with additions to optimize concrete mixtures.

iv. From the quadratic regression models found to be significant by ANOVA, it was possible to identify optimum CNT contents of between 0.045% and 0.123%, one for each property. The R^2 ranges from 41.06% to 79.77%, indicating that the models explain partially the properties' variability (P, WA, CS, TS, and UPV). Further studies must be conducted to improve the regression models' adjustment quality and help assess the benefits of incorporating CNT into concrete.

These conclusions highlight the possibility of developing regression models similar to those proposed in this study in future research covering other concrete types, considering different dosages, addition types and contents, and other relevant factors. Furthermore, these findings point towards a future direction for the construction industry, where the choice of materials and methods is as much about efficacy as it is about scalability and practicality in diverse application contexts. It is essential to highlight that the findings of this study are restricted to the analysis of concrete samples containing up to 0.10% of CNT pre-dispersed in the cement particles. Different dosages and dispersion techniques will require additional investigations for a more comprehensive understanding.

Acknowledgements

The authors thank Coordenação de Aperfeiçoamento de Pessoal de Nível Superior (CAPES, Finance Code 001), Centro Federal de Educação Tecnológica de Minas Gerais (CEFET-MG), and Laboratoire de Mécanique Paris-Saclay (LMPS) for funding this research.

References

[1] K. Thangapandi, R. Anuradha, N. Archana, P. Muthuraman, O. Awoyera Paul, R. Gobinath, Experimental Study on Performance of Hardened Concrete Using Nano Materials, KSCE Journal of Civil Engineering 24 (2020) 596–602. https://doi.org/10.1007/s12205-020-0871-y.

[2] A. Khitab, S. Ahmad, R.A. Khushnood, S.A. Rizwan, G.A. Ferro, L. Restuccia, M. Ali, I. Mehmood, Fracture toughness and failure mechanism of high performance concrete incorporating carbon nanotubes, Frattura Ed Integrita Strutturale 11 (2017) 238–248. https://doi.org/10.3221/IGF-ESIS.42.26.

[3] E.D. Reis, H.C. Gomes, R.C. de Azevedo, F.S.J. Poggiali, A.C.D.S. Bezerra, Bonding of Carbon Steel Bars in Concrete Produced with Recycled Aggregates: A Systematic Review of the Literature, C-Journal of Carbon Research 8 (2022). https://doi.org/10.3390/c8040076.

[4] A. Ebrahim, S. Kandasamy, The effect of using multi-walled carbon nanotubes on the mechanical properties of concrete: a review, Innovative Infrastructure Solutions 8 (2023) 1–13. https://doi.org/10.1007/s41062-023-01219-1.

[5] P. Zhang, S. Wei, J. Wu, Y. Zhang, Y. Zheng, Investigation of mechanical properties of PVA fiber-reinforced cementitious composites under the coupling effect of wet-thermal and chloride salt environment, Case Studies in Construction Materials 17 (2022) e01325. https://doi.org/10.1016/j.cscm.2022.e01325.

[6] D. Hwangbo, D.H. Son, H. Suh, J. Sung, B. Il Bae, S. Bae, H. So, C.S. Choi, Effect of nanomaterials (carbon nanotubes, nano-silica, graphene oxide) on bond behavior between concrete and reinforcing bars, Case Studies in Construction Materials 18 (2023) e02206. https://doi.org/10.1016/j.cscm.2023.e02206.

[7] S. Hong, J. Choi, S. Yoo, Y. Yoon, Developments in the Built Environment Structural benefits of using carbon nanotube reinforced high-strength lightweight concrete beams, Developments in the Built Environment 16 (2023) 100234. https://doi.org/10.1016/j.dibe.2023.100234.

[8] P. Van Tonder, T.T. Mafokoane, Effects of multi-walled carbon nanotubes on strength and interfacial transition zone of concrete, in: Construction Materials and Structures, IOS Press, 2014: pp. 718–727.

[9] D.-Y. Yoo, I. You, S.-J. Lee, Electrical and piezoresistive sensing capacities of cement paste with multi-walled carbon nanotubes, Archives of Civil and Mechanical Engineering 18 (2018) 371–384. https://doi.org/10.1016/j.acme.2017.09.007.

[10] B. Peng, M. Locascio, P. Zapol, S. Li, S.L. Mielke, G.C. Schatz, H.D. Espinosa, Measurements of near-ultimate strength for multiwalled carbon nanotubes and irradiation-induced crosslinking improvements, Nat Nanotechnol 3 (2008). https://doi.org/10.1038/nnano.2008.211.

[11] L. Lu, D. Ouyang, W. Xu, Mechanical properties and durability of ultra high strength concrete incorporating multi-walled carbon nanotubes, Materials 9 (2016). https://doi.org/10.3390/ma9060419.

[12] S.K. Adhikary, Ž. Rudžionis, S. Tučkutė, D.K. Ashish, Effects of carbon nanotubes on expanded glass and silica aerogel based lightweight concrete, Sci Rep 11 (2021). https://doi.org/10.1038/s41598-021-81665-y.
[13] J.M. Makar, G.W. Chan, Growth of cement hydration products on single-walled carbon nanotubes, Journal of the American Ceramic Society 92 (2009) 1303–1310. https://doi.org/10.1111/j.1551-2916.2009.03055.x.
[14] S. Xu, J. Liu, Q. Li, Mechanical properties and microstructure of multi-walled carbon nanotube-reinforced cement paste, Constr Build Mater 76 (2015) 16–23. https://doi.org/10.1016/j.conbuildmat.2014.11.049.
[15] M.S. Konsta-Gdoutos, P.A. Danoglidis, M.G. Falara, S.F. Nitodas, Fresh and mechanical properties, and strain sensing of nanomodified cement mortars: The effects of MWCNT aspect ratio, density and functionalization, Cem Concr Compos 82 (2017) 137–151. https://doi.org/10.1016/j.cemconcomp.2017.05.004.
[16] C.G.N. Marcondes, M.H.F. Medeiros, Análisis de dispersión de nanotubos de carbono en concretos de cemento Portland, Revista ALCONPAT 6 (2016).
[17] V. Vilela Rocha, P. Ludvig, Nanocomposites Prepared by a Dispersion of CNTs on Cement Particles, Architecture, Civil Engineering, Environment 11 (2018) 73–77. https://doi.org/10.21307/acee-2018-024.
[18] A. Carriço, J.A.A. Bogas, A. Hawreen, M. Guedes, Durability of multi-walled carbon nanotube reinforced concrete, Constr Build Mater 164 (2018) 121–133. https://doi.org/10.1016/j.conbuildmat.2017.12.221.
[19] V. Parvaneh, S.H. Khiabani, Mechanical and piezoresistive properties of self-sensing smart concretes reinforced by carbon nanotubes, Mechanics of Advanced Materials and Structures 26 (2019) 993–1000. https://doi.org/10.1080/15376494.2018.1432789.
[20] A. Hawreen, J.A. Bogas, R. Kurda, Mechanical Characterization of Concrete Reinforced with Different Types of Carbon Nanotubes, Arab J Sci Eng 44 (2019) 8361–8376. https://doi.org/10.1007/s13369-019-04096-y.
[21] M.O. Mohsen, M.S. Al Ansari, R. Taha, N. Al Nuaimi, A.A. Taqa, Carbon nanotube effect on the ductility, flexural strength, and permeability of concrete, J Nanomater 2019 (2019). https://doi.org/10.1155/2019/6490984.
[22] A. Hassan, H. Elkady, I.G. Shaaban, Effect of Adding Carbon Nanotubes on Corrosion Rates and Steel-Concrete Bond, Sci Rep 9 (2019). https://doi.org/10.1038/s41598-019-42761-2.
[23] S.E. Mohammadyan-Yasouj, A. Ghaderi, Experimental investigation of waste glass powder, basalt fibre, and carbon nanotube on the mechanical properties of concrete, Constr Build Mater 252 (2020) 119115. https://doi.org/10.1016/j.conbuildmat.2020.119115.
[24] M.R. Irshidat, Bond strength evaluation between steel rebars and carbon nanotubes modified concrete, Case Studies in Construction Materials 14 (2021). https://doi.org/10.1016/j.cscm.2020.e00477.
[25] E.D. Reis, L.A. Borges, J.S.F. Camargos, F. Gatuingt, F.S.J. Poggiali, A.C.S. Bezerra, A systematic review on the engineering properties of concrete with carbon nanotubes, Journal of the Brazilian Society of Mechanical Sciences and Engineering (2023). https://doi.org/10.1007/s40430-023-04117-w.
[26] I. Sadrinejad, R. Madandoust, M.M. Ranjbar, The mechanical and durability properties of concrete containing hybrid synthetic fibers, Constr Build Mater 178 (2018) 72–82. https://doi.org/10.1016/j.conbuildmat.2018.05.145.
[27] C. Ince, B.M.H. Shehata, S. Derogar, R.J. Ball, Towards the development of sustainable concrete incorporating waste tyre rubbers: A long-term study of

physical, mechanical & durability properties and environmental impact, J Clean Prod 334 (2022) 130223. https://doi.org/10.1016/j.jclepro.2021.130223.
[28] D.A. Freedman, Statistical models: theory and practice, 7th ed., Nova York, 2009.
[29] S. Ahmad, S.A. Alghamdi, A statistical approach to optimizing concrete mixture design, The Scientific World Journal 2014 (2014). https://doi.org/10.1155/2014/561539.
[30] R. Perumal, Correlation of Compressive Strength and Other Engineering Properties of High-Performance Steel Fiber–Reinforced Concrete, Journal of Materials in Civil Engineering 27 (2015) 1–8. https://doi.org/10.1061/(asce)mt.1943-5533.0001050.
[31] ABNT, NBR 16697: Cimento Portland - Requisitos, ABNT (2018).
[32] EN197:2011, Cement – Part 1 : Composition , specifications and conformity criteria for, 1 (2011) 1–30.
[33] ABNT, NBR NM 248: Agregados – Determinação da composição granulométrica, ABNT (2003).
[34] ABNT, NBR 9776: Agregados – Determinação da massa específica de agregados miúdos por meio do frasco de Chapman, ABNT (1987).
[35] ABNT, NBR 16372: Cimento Portland e outros materiais em pó – Determinação da finura pelo método de permeabilidade ao ar (método de Blaine), ABNT (2015) 11.
[36] ABNT, NBR 16607: Cimento Portland – Determinação dos tempos de pega, ABNT (2018) 4.
[37] ABNT, NBR 7215: Cimento Portland – Determinação da resistência à compressão de corpos de provas cilíndricos, ABNT (2019) 18.
[38] NanoView. Nanotubos de Carbono de Múltiplas Paredes. NanoView Nanotecnologia: Ficha Técnica Do Nanomaterial 2022:1.
[39] EMFAL. Álcool isopropílico 100 °INPM Farmacêutico EP. EMFAL: Ficha de Informação Técnica 2019:2.
[40] S. Chuah, W. Li, S.J. Chen, J.G. Sanjayan, W.H. Duan, Investigation on dispersion of graphene oxide in cement composite using different surfactant treatments, Constr Build Mater 161 (2018) 519–527. https://doi.org/10.1016/j.conbuildmat.2017.11.154.
[41] ABNT, NBR 8953: Concreto para fins estruturais: Classificação por grupo de resistência, ABNT (2015) 3.
[42] ABNT, NBR 5738: Concreto - Procedimento para moldagem e cura de corpos de prova, ABNT (2015) 13.
[43] ABNT, NBR 5739: Concreto - Ensaio de compressão de corpos de prova cilíndricos, ABNT (2018) 13.
[44] ABNT, NBR 7222: Concreto e argamassa - Determinação da resistência à tração por compressão diametral de corpos de prova cilíndricos, ABNT (2011) 9.
[45] ABNT, NBR 8522-1: Concreto endurecido - Determinação dos módulos de elasticidade e de deformação, ABNT (2021).
[46] ASTM, ASTM C215-8: Standard test method for fundamental transverse, longitudinal, and torsional frequencies of concrete specimens, ASTM 7 (2017).
[47] BS, BS 1881: Testing concrete. Part 209: Recommendations for the measurement of dynamic modulus of elasticity, BS (1990) 8.
[48] ABNT, NBR 9778 versão 2: Argamassa e concreto endurecidos – Determinação da absorção de água, índice de vazios e massa específica, ABNT (2009).

[49] N. Venkata Sairam Kumar, Effect of sulfuric and hydrochloric acid solutions on crushed rock dust concrete, Mater Today Proc 46 (2021) 509–513. https://doi.org/10.1016/j.matpr.2020.10.691.
[50] H. Boudjehm, F. Bouteldja, Z. Nafa, R. Bendjaiche, Hardened properties of pre-cracked concrete incorporating metakaolin and crushed blast furnace slag as an additional blend material, Constr Build Mater 352 (2022) 129009. https://doi.org/10.1016/j.conbuildmat.2022.129009.
[51] D. Sinkhonde, R.O. Onchiri, W.O. Oyawa, J.N. Mwero, Durability and water absorption behaviour of rubberised concrete incorporating burnt clay brick powder, Cleaner Materials 4 (2022) 100084. https://doi.org/10.1016/j.clema.2022.100084.
[52] L. Wu, G. Huang, W.V. Liu, Methods to evaluate resistance of cement-based materials against microbially induced corrosion: A state-of-the-art review, Cem Concr Compos 123 (2021) 104208. https://doi.org/10.1016/j.cemconcomp.2021.104208.
[53] N. Singh, P. Kumar, P. Goyal, Reviewing the behaviour of high volume fly ash based self compacting concrete, Journal of Building Engineering 26 (2019) 100882. https://doi.org/10.1016/j.jobe.2019.100882.
[54] ABNT, NBR 8802: Concreto endurecido – Determinação da velocidade de propagação de onda ultrassônica, ABNT (2019) 11.
[55] International Atomic Energy Agency, Guidebook on non-destructive testing of concrete structures, Industrial Applications and Chemistry Section, IAEA 17 (2002) 231.
[56] F.A. Wenner, A method of measuring earth resistivity, Bulletin of the Bureau of Standards, US Bureau of Standards 12 (1915) 469–478.
[57] P. Langford, J. Broomfield, Monitoring the corrosion of reinforcing steel, Construction Repair 1 (1987) 32–36.
[58] E. P. Figueiredo, Ensaios eletroquímicos para avaliação da corrosão das armaduras, I Simpósio Sobre Ensaios Não Destrutivos Para Estruturas de Concreto (2010) 42.
[59] D.C. Mongomery, Montgomery: Design and Analysis of Experiments, John Willy & Sons (2017).
[60] N.S. Piro, A. Salih, S.M. Hamad, R. Kurda, Comprehensive multiscale techniques to estimate the compressive strength of concrete incorporated with carbon nanotubes at various curing times and mix proportions, Journal of Materials Research and Technology 15 (2021) 6506–6527. https://doi.org/10.1016/j.jmrt.2021.11.028.
[61] D. Yang, P. Xu, A. Zaman, T. Alomayri, M. Houda, A. Alaskar, M.F. Javed, Compressive strength prediction of concrete blended with carbon nanotubes using gene expression programming and random forest: hyper-tuning and optimization, Journal of Materials Research and Technology 24 (2023) 7198–7218. https://doi.org/10.1016/j.jmrt.2023.04.250.
[62] A. Hawreen, J.A. Bogas, Creep, shrinkage and mechanical properties of concrete reinforced with different types of carbon nanotubes, Constr Build Mater 198 (2019) 70–81. https://doi.org/10.1016/j.conbuildmat.2018.11.253.
[63] M.S. Konsta-Gdoutos, P.A. Danoglidis, S.P. Shah, High modulus concrete: Effects of low carbon nanotube and nanofiber additions, Theoretical and Applied Fracture Mechanics 103 (2019). https://doi.org/10.1016/j.tafmec.2019.102295.
[64] U. Abinayaa, D. Chetha, S. Chathuska, N. Praneeth, R. Vimantha, K.K. Wijesundara, Improving the properties of concrete using carbon nanotubes, in:

SAITM Research Symposium on Engineering Advancements, 2014: pp. 201–204.
[65] M.B. Asil, M.M. Ranjbar, Hybrid effect of carbon nanotubes and basalt fibers on mechanical, durability, and microstructure properties of lightweight geopolymer concretes, Constr Build Mater 357 (2022). https://doi.org/10.1016/j.conbuildmat.2022.129352.
[66] X. Song, J. Zhang, S. Shang, Mechanical properties of early-age concrete reinforced with multi-walled carbon nanotubes, Magazine of Concrete Research 69 (2017) 683–693. https://doi.org/10.1680/jmacr.16.00424.
[67] X.B. Song, qi Cai, Y.Q. Li, C.Z. Li, Bond behavior between steel bars and carbon nanotube modified concrete, Constr Build Mater 255 (2020). https://doi.org/10.1016/j.conbuildmat.2020.119339.
[68] M. Jung, Y. soon Lee, S.G. Hong, J. Moon, Carbon nanotubes (CNTs) in ultra-high performance concrete (UHPC): Dispersion, mechanical properties, and electromagnetic interference (EMI) shielding effectiveness (SE), Cem Concr Res 131 (2020) 106017. https://doi.org/10.1016/j.cemconres.2020.106017.
[69] M. Jung, J. Park, S. Hong, J. Moon, The critical incorporation concentration (CIC) of dispersed carbon nanotubes for tailoring multifunctional properties of ultra-high performance concrete (UHPC), Journal of Materials Research and Technology 17 (2022) 3361–3370. https://doi.org/10.1016/j.jmrt.2022.02.103.
[70] A.S. Ali, A.A.M. Al-Shaar, A.A. Shakir, Electrical properties of fibrous self-compacting concrete reinforced with different types of fibers, Mater Today Proc 42 (2021) 2012–2017. https://doi.org/10.1016/j.matpr.2020.12.252.
[71] D.-H. Son, D. Hwangbo, H. Suh, B.-I. Bae, S. Bae, C.-S. Choi, Mechanical properties of mortar and concrete incorporated with concentrated graphene oxide, functionalized carbon nanotube, nano silica hybrid aqueous solution, Case Studies in Construction Materials 18 (2023) e01603. https://doi.org/10.1016/j.cscm.2022.e01603.
[72] J. Xiao, Z. Lv, Z. Duan, C. Zhang, Pore structure characteristics, modulation and its effect on concrete properties: A review, Constr Build Mater 397 (2023) 132430. https://doi.org/10.1016/j.conbuildmat.2023.132430.
[73] Y.B. Wang, J.Y.R. Liew, S.C. Lee, D.X. Xiong, Experimental study of ultra-high-strength concrete under triaxial compression, ACI Mater J 113 (2016) 105–112. https://doi.org/10.14359/51688071.
[74] R. Kumar, B. Bhattacharjee, Porosity, pore size distribution and in situ strength of concrete, Cem Concr Res 33 (2003) 155–164. https://doi.org/10.1016/S0008-8846(02)00942-0.
[75] M.A. Vicente, D.C. González, J. Mínguez, M.A. Tarifa, G. Ruiz, R. Hindi, Influence of the pore morphology of high strength concrete on its fatigue life, Int J Fatigue 112 (2018) 106–116. https://doi.org/10.1016/j.ijfatigue.2018.03.006.
[76] J. Huang, Y. Zhang, Y. Sun, J. Ren, Z. Zhao, J. Zhang, Evaluation of pore size distribution and permeability reduction behavior in pervious concrete, Constr Build Mater 290 (2021) 123228. https://doi.org/10.1016/j.conbuildmat.2021.123228.
[77] M. Thanmanaselvi, V. Ramasamy, A study on durability characteristics of nano-concrete, Mater Today Proc 80 (2023) 2360–2365. https://doi.org/10.1016/j.matpr.2021.06.349.
[78] Q. Fu, Z. Zhou, Z. Wang, J. Huang, D. Niu, Insight into dynamic compressive response of carbon nanotube/carbon fiber-reinforced concrete, Cem Concr Compos 129 (2022). https://doi.org/10.1016/j.cemconcomp.2022.104471.

[79] G. Liu, D. Kan, S. Cindy Cao, Z. Chen, Q. Lyu, Effect of multi-walled carbon nanotube on reactive powder concrete (RPC) performance in sulfate dry-wet cycling environment, Constr Build Mater 342 (2022) 128075. https://doi.org/10.1016/j.conbuildmat.2022.128075.
[80] M. Jung, J. Park, S. gul Hong, J. Moon, The critical incorporation concentration (CIC) of dispersed carbon nanotubes for tailoring multifunctional properties of ultra-high performance concrete (UHPC), Journal of Materials Research and Technology 17 (2022) 3361–3370. https://doi.org/10.1016/j.jmrt.2022.02.103.
[81] M.S. Hasan, S. Setunge, D.W. Law, T.C.K. Molyneaux, Predicting life expectancy of concrete septic tanks exposed to sulfuric acid attack, Magazine of Concrete Research 65 (2013) 793–801. https://doi.org/10.1680/macr.12.00231.
[82] M. O'Connell, C. McNally, M.G. Richardson, Biochemical attack on concrete in wastewater applications: A state of the art review, Cem Concr Compos 32 (2010) 479–485. https://doi.org/10.1016/j.cemconcomp.2010.05.001.
[83] A. Mehta, R. Siddique, Sulfuric acid resistance of fly ash based geopolymer concrete, Constr Build Mater 146 (2017) 136–143. https://doi.org/10.1016/j.conbuildmat.2017.04.077.
[84] E. Mohseni, W. Tang, H. Cui, Chloride diffusion and acid resistance of concrete containing zeolite and tuff as partial replacements of cement and sand, Materials 10 (2017). https://doi.org/10.3390/ma10040372.
[85] S.A.M. Rad, A. Modarres, Durability properties of non-air entrained roller compacted concrete pavement containing coal waste ash in presence of de-icing salts, Cold Reg Sci Technol 137 (2017) 48–59. https://doi.org/10.1016/j.coldregions.2017.02.006.
[86] K. Lim, N. Lee, G. Ryu, K. Koh, K. Kim, Electrical Characteristics of Ultra-High-Performance Concrete Containing Carbon-Based Materials, Applied Sciences (Switzerland) 12 (2022). https://doi.org/10.3390/app12157858.
[87] A. Hawreen, J.A. Bogas, Influence of carbon nanotubes on steel–concrete bond strength, Materials and Structures/Materiaux et Constructions 51 (2018). https://doi.org/10.1617/s11527-018-1279-8.